J Membrane Biol (2013) 246:705–715
DOI 10.1007/s00232-013-9590-3

# Functional Characterization of SdcF from *Bacillus licheniformis*, a Homolog of the SLC13 $Na^+$/Dicarboxylate Transporters

**Ana M. Pajor · Nina N. Sun · Alva Leung**

Received: 1 May 2013 / Accepted: 10 August 2013 / Published online: 25 August 2013


**Abstract** The SdcF transporter from *Bacillus licheniformis* (gene *BL02343*) is a member of the divalent anion sodium symporter (DASS)/SLC13 family that includes $Na^+$/dicarboxylate transporters from bacteria to humans. SdcF was functionally expressed in *Escherichia coli* (BL21) and assayed in right side out membrane vesicles. ScdF catalyzed the sodium-coupled transport of succinate and α-ketoglutarate. Succinate transport was strongly inhibited by malate, fumarate, tartrate, oxaloacetate and L-aspartate. Similar to the other DASS transporters, succinate transport by SdcF was inhibited by anthranilic acids, *N*-(*p*-amylcinnamoyl) anthranilic acid and flufenamate. SdcF transport was cation-dependent, with a $K_{0.5}$ for sodium of ~1.5 mM and a $K_{0.5}$ for $Li^+$ of ~40 mM. Succinate transport kinetics by SdcF were sigmoidal, suggesting that SdcF may contain two cooperative substrate binding sites. The results support an ordered binding mechanism for SdcF in which sodium binds first and succinate binds last. We conclude that SdcF is a secondary active transporter for four- and five-carbon dicarboxylates that can use $Na^+$ or $Li^+$ as a driving cation.

**Keywords** Sodium · Succinate · Lithium · Transport · DASS family

**Abbreviations**

| | |
|---|---|
| ACA | *N*-(*p*-amylcinnamoyl) anthranilic acid |
| AKG | Alpha-ketoglutarate |
| DASS | Divalent anion sodium symporter family |
| IPTG | Isopropyl-β-D-thiogalactopyranoside |
| KPi | Potassium phosphate buffer |
| MTSET | [2-(Trimethylammonium)ethyl] methanethiosulfonate |
| NAA | *N*-acetyl L-aspartate |
| OAA | Oxaloacetate |

A. M. Pajor (✉) · N. N. Sun · A. Leung
Skaggs School of Pharmacy and Pharmaceutical Sciences, University of California-San Diego, La Jolla, CA 92093-0718, USA
e-mail: apajor@ucsd.edu

## Introduction

The divalent anion sodium symporter (DASS) family includes sodium-coupled transporters for citric acid cycle intermediates, such as succinate and citrate (Prakash et al. 2003). The mammalian members of this family form the SLC13 family and include the $Na^+$/dicarboxylate cotransporters (NaDC1, NaDC3 and NaCT) that use the energy available from the transmembrane electrochemical gradient for sodium to perform concentrative transport of citric acid cycle intermediates (Pajor 2006). All of the mammalian transporters interact with lithium, which can either substitute partially for sodium or inhibit transport by competing with sodium at a high-affinity cation binding site (Pajor et al. 1998).

Several prokaryotic members of the DASS family have been sequenced and functionally characterized: SdcS from *Staphylococcus aureus*, DccT from *Corynebacterium glutamicum* and SdcL from *Bacillus licheniformis* (Hall and Pajor 2005; Strickler et al. 2009; Youn et al. 2008). All are sodium-coupled transporters that carry four-carbon dicarboxylate substrates, including succinate, fumarate and malate, with relatively high affinity. These nutrient transporters are important for the physiology of the microorganisms in which they are expressed (Ebbighausen et al. 1991; Teramoto et al. 2008), and they can serve as model systems for the study of the mammalian homologs. Furthermore, the prokaryotic transporters can be readily

overexpressed in *Escherichia coli*, which allows detailed biochemical and functional characterization. Recently, the structure of the *Vibrio cholerae* $Na^+$/dicarboxylate symporter VcINDY from the DASS family was solved in an inward-facing conformation (Mancusso et al. 2012).

We report the functional characterization of the SdcF $Na^+$/dicarboxylate transporter from *B. licheniformis*, a gram-positive bacterium found in soil and used in industrial applications to produce enzymes (Rey et al. 2004; Williams et al. 1990). SdcF was identified as a DASS family member by sequence comparison. SdcF is 49 % identical in sequence to SdcL from *B. licheniformis* and has many similarities in functional properties. One surprising finding was that SdcF can transport succinate equally well at high concentrations of lithium or sodium, although the affinity for lithium was lower than that for sodium. Our results also support an ordered binding mechanism for SdcF in which sodium binds first and succinate binds last.

## Materials and Methods

### Bacterial Strains and Plasmids

*Escherichia coli* strain DH5α ($F^-$ Φ80*lac*ZΔM15 Δ[*lac*ZYA-*arg*F] U169 *rec*A1 *end*A1 *hsd*R17 [$rK^-$, $mK^+$] *pho*A *sup*E44 λ-*thi*-1 *gyr*A96 *rel*A1 [Invitrogen, Carlsbad, CA]) was used for all cloning steps. *E. coli* strain BL21 ($F^-$ *ompT hsdS*$_B$ [$r_B^-$ $m_B^-$] *gal dcm* [Novagen, Madison, WI]) was used as a host for expression and function of plasmid-encoded SdcF, SdcS and DccT. *E. coli* strain C41 (DE3) ($F^-$ *ompT hsdS*$_B$ [$r_B^-$ $m_B^-$] *gal dcm* [DE3] [Lucigen, Middleton, WI]) was used as a host for expression of SdcL.

The *BL02343* gene coding for the SdcF transporter (GenBank accession number NC006270, locus YP077725 and AAU22344) was amplified from *B. licheniformis* genomic DNA (ATCC 14580) by PCR and cloned into plasmid pQE-80L (Qiagen, Valencia, CA) via introduced restriction sites *Bam*HI and *Kpn*I. The recombinant plasmid (pQE-80L/SdcF) encodes SdcF with an N-terminal mRGS(H)$_6$GS amino acid extension and places BL02343 expression under the control of a T5 promoter/lac operator element. The *dccT* gene [Genbank accession number BA000036.3, locus gc10225 and BAB97618.1 (Youn et al. 2008)] was amplified from *C. glutamicum* genomic DNA (ATCC 13032) using a similar PCR approach and cloned into pQE-80L. Plasmids pQE-80L/SdcS and pQE-80L/SdcL were described previously (Hall and Pajor 2005; Strickler et al. 2009).

### Preparation of Right Side out Membrane Vesicles

The pQE-80L/SdcF construct was transformed into *E. coli* BL21 cells. Overnight cultures of transformed *E. coli* BL21 cells were diluted 1:100 to inoculate 500 ml of yeast extract tryptone (YT) medium containing 50 μg/ml carbenecillin. Cells were grown at 37 °C until the $OD_{660}$ reached 0.4–0.6. Isopropyl-β-D-thiogalactopyranoside (IPTG) was added to a final concentration of 150 μM, and cell growth was continued for another 2 h. Cells were harvested by centrifugation at 2,000×*g* for 15 min at 4 °C and then used for preparation of right side out (RSO) inner membrane vesicles, as described previously (Joshi and Pajor 2009). Washed cells were then treated with a combination of lysozyme and osmotic lysis, followed by differential centrifugation to purify the RSO membrane vesicles. The vesicles were resuspended in 100 mM KPi buffer, pH 7 (SdcF, SdcS, DccT), or 100 mM Tris/MES buffer, pH 7 (SdcL); quick frozen in liquid nitrogen; and stored in aliquots at −80 °C until use. For some reason, SdcL vesicles resuspended in KPi buffer were inactive. However, vesicles from the same membrane preparation in KPi buffer were washed, pelleted and resuspended in Tris/MES buffer, after which they exhibited full activity (results not shown).

### Succinate Transport Assays

Uptake of [$^{14}$C]succinate by RSO vesicles containing SdcF was measured using a rapid filtration assay at room temperature (Joshi and Pajor 2009). For each assay, 40 μl of $Na^+$ or choline transport buffer containing 20 μM [$^{14}$C]succinate (62.7 mCi/mmol; Moravek, Brea, CA) was placed in the bottom of a 5-ml polystyrene tube (Falcon; BD Biosciences, San Jose, CA), and a 10-μl drop of RSO vesicles was added to the side of the tube. The $Na^+$ transport buffer consisted of 12.5 mM NaCl, 87.5 mM choline Cl and 50 mM MOPS, pH adjusted to 7 with Tris base; and the choline transport buffer contained 100 mM choline Cl and 50 mM MOPS, pH adjusted to 7 with Tris base. Unless otherwise noted, the final concentration of $Na^+$ in the assays was 10 mM. Transport was initiated by vortexing the two drops together. The reaction was terminated after the appropriate time, usually 30 s, with 1 ml ice-cold choline buffer, filtered immediately through a Millipore (Billerica, MA) filter (0.45 μm pore size, type HAWP) with suction, and washed once with 4 ml cold choline buffer. For a time 0 point, the stop solution was added to the transport buffer before it was mixed with the RSO vesicles. The radioactivity retained by the filters was measured by liquid scintillation counting.

For experiments testing the inhibition of succinate transport by potential dicarboxylate substrates, a final concentration of 1 mM of the test inhibitor was added together with 20 μM [$^{14}$C]succinate in the transport solution. In experiments testing the effect of different monovalent cations, the transport buffer contained 10 mM (final

concentration) NaCl or other chloride salts with 70 mM choline Cl and 50 mM MOPS, pH 7, or 80 mM NaCl or other chloride salts, 50 mM MOPS, pH 7. Sodium activation of succinate uptake was determined by replacing NaCl with choline Cl up to a final concentration of 10 mM in the transport solution. $Li^+$ activation was measured using LiCl up to a final concentration of 80 mM, similar to the $Na^+$ activation experiment, or with higher concentrations of $Li^+$ up to 240 mM (made using combinations of 300 mM LiCl or choline Cl/50 mM MOPS). Apparent kinetic constants ($K_{0.5}$, $V_{max}$) for cation activation and succinate transport were determined by fitting initial transport rates (10 s) to the Hill equation, $v = (V_{max}[S]^n)/(K_{0.5}^n + [S]^n)$, where n represents the Hill coefficient, using nonlinear regression analysis (SigmaPlot 10.0; Systat Software, Chicago, IL). Throughout the text, the half-saturation constant derived from Hill analysis is $K_{0.5}$, whereas the half-saturation constant from Michaelis–Menten analysis is $K_m$.

### Immunoblot Analysis

Washed BL21 cells were diluted with sample buffer (final concentration 50 mM Tris–HCl [pH 7], 10 % glycerol, 4 % SDS, 2 % β-mercaptoethanol, 0.1 mg/ml Coomassie blue R-250) and heated at 55 °C for 15 min. Proteins were separated by tricine SDS-PAGE with 7.5 % (w/v) acrylamide and transferred to nitrocellulose membranes as described (Hall and Pajor 2005; Joshi and Pajor 2009). Blots were incubated with a 1:2,000 dilution of mouse monoclonal antibody (RGS-His antibody, Qiagen), followed by a 1:5,000 dilution of horseradish peroxidase–conjugated anti-mouse immunoglobulin G antibody (Jackson ImmunoResearch Laboratories, West Grove, PA). Antibody binding was detected with the Supersignal West Pico chemiluminescent substrate kit (Pierce, Rockford, IL). Images were captured with a Kodak (Rochester, NY) Image Station 4000R.

### Protein Determination

The protein concentration of the membrane vesicles was measured using the Bio Rad (Hercules, CA) protein assay kit according the manufacturer's direction. The protein standard used was bovine plasma γ-globulin.

## Results

### Cloning and Functional Expression

The *BL02343* gene from *B. licheniformis* was identified as a member of the DASS/SLC13 family by sequence comparison. The protein encoded by *BL02343* was named SdcF (Genbank AAU22344), and it has 474 amino acids with a predicted molecular mass of 51 kDa. The amino acid sequence of SdcF is 49 % identical to that of SdcL, the previously identified $Na^+$/dicarboxylate transporter from *B. licheniformis* (*BL01224* gene; Genbank YP_077725.1) (Strickler et al. 2009), which has 546 amino acids and a longer N-terminal tail (Fig. 1). SdcF is 34 % identical to the human $Na^+$/dicarboxylate transporter NaDC1 (SLC13A2; Genbank AAA98504). Furthermore, the amino acid sequence of SdcF is 43 % identical to SdcS from *S. aureus* (BAB58078) (Hall and Pajor 2005), 38 % identical to DccT from *C. glutamicum* (BAB97618.1) (Youn et al. 2008) and 35 % identical to VcINDY from *V. cholerae* (AAF95939) (Mancusso et al. 2012) (Fig. 1). Note that *C. glutamicum* contains two dicarboxylate transporters, DccT (Youn et al. 2008) and DcsT (Teramoto et al. 2008), that differ by only two amino acids at positions 512 and 514 (see alignments [Strickler et al. 2009]). The sequence alignment of SdcF with the bacterial DASS transporters (Fig. 1) shows the positions of transmembrane helices and hairpin loops based on the crystal structure of VcINDY (Mancusso et al. 2012). Regions of high sequence conservation are found in TM2, TM3 and TM4b and the cytoplasmic surface helix H4c, TM5a and b, TM9b and TM10b. The $HP_{in}$ and $HP_{out}$ hairpin loops that contain sodium and substrate binding residues are also highly conserved among the bacterial DASS transporters (Fig. 1).

SdcF was expressed in *E. coli* (BL21) for functional characterization. Western blots showed a main protein band of around 36–40 kDa and occasionally a lower band of 21 kDa after protein induction with IPTG. As shown in Fig. 2a, there was similar SdcF protein abundance with IPTG concentrations of 150–500 μM, although the lower concentration of 150 μM seemed to give more consistent results (results not shown). The time course of SdcF induction before and after addition of IPTG is shown in Fig. 2b. The induction appeared complete after 1 h. Therefore, experiments in this study were done using a 2-h induction period with 150 μM IPTG.

### Time Course of Succinate Transport in RSO Vesicles

Figure 3 shows the succinate transport activity over time in RSO membrane vesicles prepared from *E. coli* (BL21) transformed with the control plasmid pQE-80L or with pQE-80L/SdcF. Transport by SdcF was sodium-dependent and showed a peak accumulation at around 1 min that decreased toward background levels by 15 min. When sodium was replaced by choline in the transport buffer, the succinate transport activity by SdcF was reduced to background levels, similar to that seen in control cells transformed with pQE-80L. Therefore, we used 10 and 30 s time points in this study as a measure of initial rates.

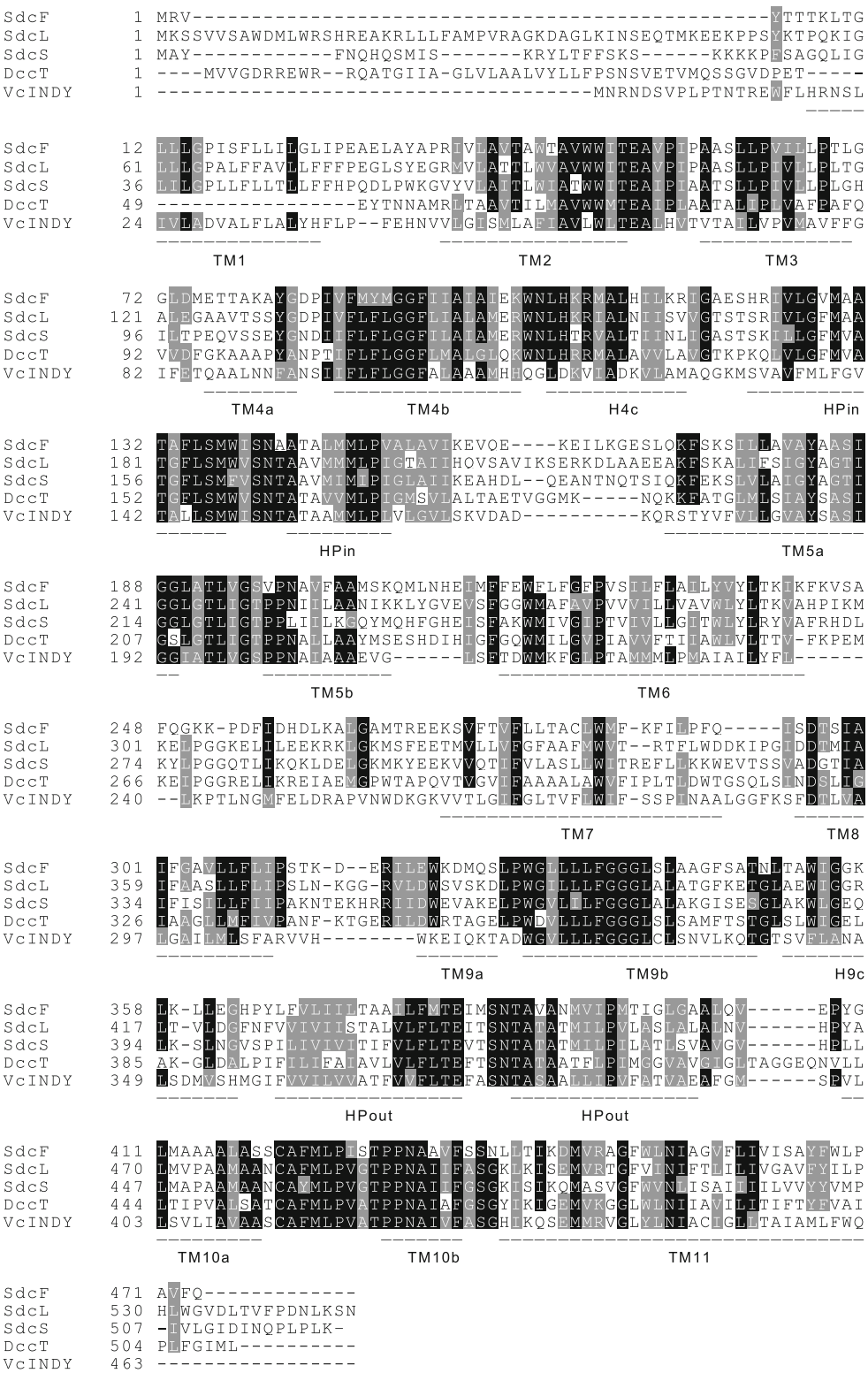


**Fig. 1** Sequence alignment of SdcF with other bacterial DASS dicarboxylate transporters. The Genbank accession numbers of the peptide sequences are SdcF (AAU22344), SdcL (YP_077725.1), SdcS (BAB58078), DccT (BAB97618.1), VcINDY (AAF95939). The alignment was made using ClustalW. The *shaded regions* represent conserved amino acids. The *underlined regions* show the positions of transmembrane helices (TM1-11), surface helices (H) and hairpin loops (HP), based on the crystal structure of VcINDY (Mancusso et al. 2012)

## Substrate Specificity

We examined the substrate specificity of SdcF in RSO membrane vesicles by inhibition of [$^{14}$C]succinate transport using 1 mM concentrations of test substrates. SdcF was strongly inhibited by four-carbon dicarboxylates: succinate, malate, fumarate, tartrate (2,3-dihydroxysuccinate) and oxaloacetate (OAA) (Fig. 4b). Transport of succinate was also inhibited more than 80 % by the amino acid L-aspartate. There was less transport inhibition, about

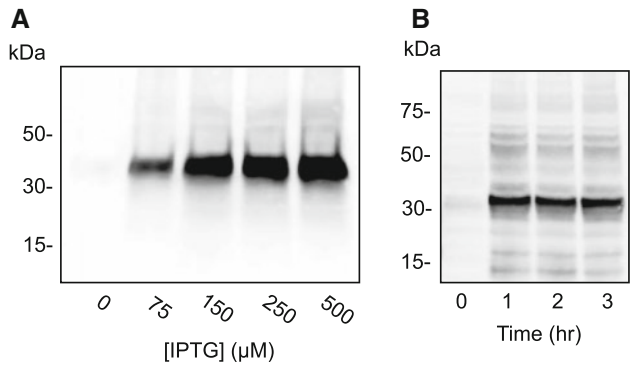


**Fig. 2** Western blots of washed *E. coli* BL21 cells expressing SdcF. Sizes of molecular mass standards (6X His protein ladder, Qiagen) are shown at the *left of each blot*. **a** BL21 transformed with pQE-80L/SdcF were grown in YT medium and treated for 2 h with different concentrations of IPTG, from 0 to 500 μM. Each lane was loaded with 10 μg protein. **b** Time course of SdcF expression in BL21 cells grown in YT medium before and after the addition of 500 μM IPTG. Each lane was loaded with 15 μg protein. Proteins were detected using the RGS-His antibody (Qiagen), a monoclonal antibody directed against the N-terminal histidine tag

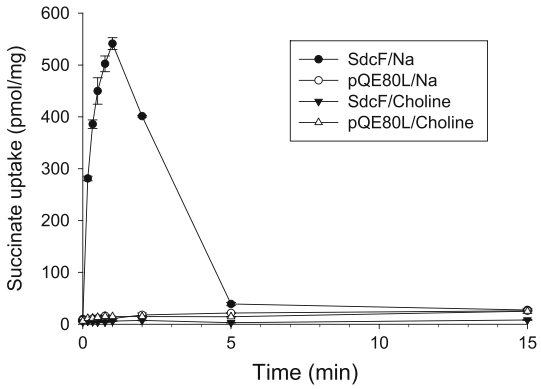


**Fig. 3** Time course of succinate transport in RSO vesicles. Transport of 20 μM [$^{14}$C]succinate was measured in buffer containing 10 mM $Na^+$/70 mM choline Cl (sodium buffer) or 80 mM choline Cl (choline) in RSO vesicles prepared from *E. coli* (BL21 strain) expressing SdcF or transformed with pQE-80L control plasmid. Uptakes were measured between 10 s and 15 min. The results shown are the mean of duplicate measurements from a single membrane preparation, with *error bars* representing the range. The data in this figure are shown without correction for background

35 %, by *N*-acetyl-L-aspartate (NAA) and α-ketoglutarate (AKG), suggesting that the affinity for these substrates is low. NAA is a substrate of the high-affinity $Na^+$/dicarboxylate cotransporter NaDC3, found in mammalian brain (Huang et al. 2000). There was no inhibition of [$^{14}$C]succinate transport by citrate. We next examined the uptake of some [$^{14}$C]-labeled substrates in RSO membrane vesicles expressing SdcF (Fig. 4b). The highest transport activity was seen with [$^{14}$C]succinate, and there was some transport of AKG, ~13 % of the activity seen with succinate, consistent with a low affinity for AKG. There was no transport activity of [$^{14}$C]citrate either at pH 7 or at pH 6 (to increase the concentration of divalent citrate). In the mammalian NaDC1, the preferred substrate is protonated citrate$^{2-}$ and transport is stimulated by acidic pH (Pajor 1995). The effects of nonsubstrate inhibitors on SdcF transport activity were also tested (Fig. 4c). The anthranilic acids *N*-(*p*-amylcinnamoyl) anthranilic acid (ACA) and flufenamate are inhibitors of SdcS and the mammalian members of the family (Pajor and Sun 2013; Pajor and Randolph 2005). Both ACA and flufenamate inhibited succinate transport in SdcF (Fig. 4c), although SdcF seemed less sensitive to both compounds compared with SdcS (Pajor and Sun 2013). We also tested the effect of (2-[trimethylammonium]ethyl) methanethiosulfonate (MTSET), which had no effect on succinate transport by SdcF. MTSET is a membrane-impermeant, cysteine-selective reagent which should react with extracellularly accessible cysteines. MTSET inhibited SdcS, which has a single cysteine at position 457; but the inhibition was seen only in inside-out membrane vesicles (Joshi and Pajor 2009). SdcF contains two endogenous cysteines: Cys-421 is conserved with SdcS and is predicted to be in the unwound portion of TM10, whereas Cys-282 is predicted to be midway through TM7 (Fig. 1). Therefore, the lack of inhibition of SdcF by MTSET shows that neither cysteine is accessible from the outside of the vesicles or that labeling of the cysteine does not have a functional effect.

The other bacterial DASS transporters studied to date seem to have similar substrate specificity profiles as SdcF. However, we found differences among the DASS transporters in their sensitivity to inhibition of [$^{14}$C]succinate transport by tartrate (Fig. 4d). We prepared RSO membrane vesicles from *E. coli* transformed with plasmids encoding SdcS, SdcL or DccT. As shown in Fig. 4d, the SdcL transporter from *B. licheniformis* was completely inhibited by 1 mM tartrate, whereas SdcS and DccT were much less sensitive. In a previous study using proteoliposomes, SdcS was not affected by tartrate but the [$^{14}$C]succinate concentration was saturating (100 μM), which could make it difficult to see inhibition by a low-affinity substrate (Hall and Pajor 2007). In the present study, there was about 25 % inhibition by tartrate in SdcS and about 47 % inhibition in DccT (Fig. 4d). Therefore, one functional difference between the bacterial DASS transporters appears to be in their binding or transport of tartrate.

## Cation Specificity

We next examined the cation specificity of SdcF by measuring succinate transport in RSO vesicles in the presence of different cations (Fig. 5). In our previous studies, we found that the succinate transport activity of SdcS and

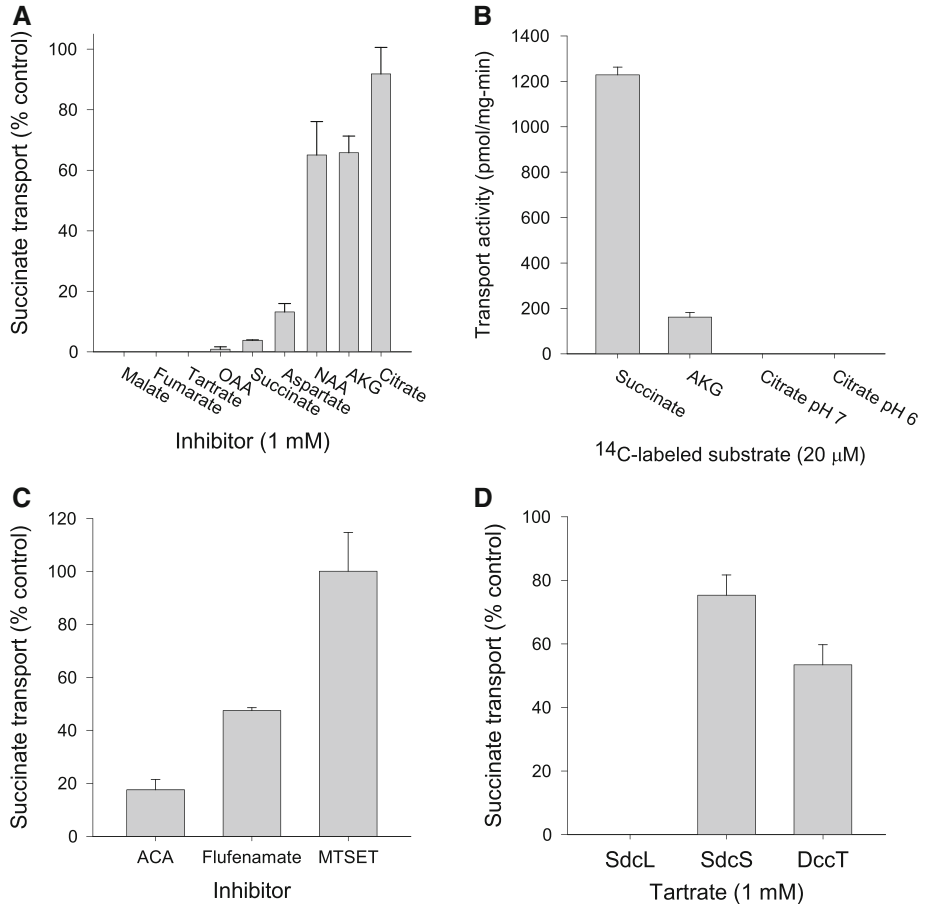


**Fig. 4** Substrate specificity of SdcF. **a** Substrate inhibition. $Na^+$-dependent [$^{14}$C]succinate transport activity was measured in the presence or absence of 1 mM test substrates in RSO vesicles expressing SdcF. The concentration of [$^{14}$C]succinate was 20 μM. The results shown are the mean of duplicate or triplicate experiments, with *error bars* showing the range or SEM, expressed as a percentage of transport in the absence of inhibitor. *OAA* oxaloacetate, *NAA* *N*-acetylaspartate, *AKG* α-ketoglutarate. **b** Substrate uptake. Transport of [$^{14}$C]-labeled substrates, 20 μM each, in RSO vesicles. 30-s uptakes were measured in buffer containing a final concentration of 10 mM $Na^+$. The results shown are means, with *error bars* showing the range ($n = 2$ experiments). **c** Inhibitors. Effect of 100 μM ACA, 100 μM flufenamate or 1 mM MTSET on [$^{14}$C]succinate transport by SdcF in RSO vesicles. Membranes were preincubated with inhibitor or vehicle (DMSO) for 10 min, followed by 30-s uptake measurement. The results shown are mean ± SEM ($n = 3$ experiments), expressed as a percentage of transport in the absence of inhibitor. **d** Tartrate inhibition of bacterial DASS transporters. $Na^+$-dependent [$^{14}$C]succinate transport activity was measured in the presence or absence of 1 mM tartrate in RSO vesicles expressing SdcL, SdcS and DccT. Conditions were the same as in **a**

SdcL was highest at ~10 mM $Na^+$ and inhibited by higher concentrations of sodium (Hall and Pajor 2005; Joshi and Pajor 2009; Strickler et al. 2009). This inhibition appears to be related to an endogenous protein in *E. coli* membranes because it has been observed also for the tyrosine transporter Tyt1 expressed in *E. coli* (Quick et al. 2006) but was not seen in purified SdcS in proteoliposomes (Hall and Pajor 2007). Similarly, when we measured the transport activity of SdcF, it was highest in 10 mM NaCl and much lower at 80 mM NaCl (Fig. 5). The transport of succinate by SdcF was observed in the presence of lithium, and the transport rate in 80 mM lithium was almost as high as that in 10 mM sodium. By comparison, succinate transport by SdcS from *S. aureus* can also be driven by lithium, but lithium can support only ~40 % of the maximal activity seen with sodium (Hall and Pajor 2005). There was no activity above background in transport buffer containing 80 mM choline Cl or 80 mM KCl (Fig. 5).

## Succinate Kinetics in Sodium

The kinetics of succinate transport in sodium were examined in vesicles expressing SdcF. In order to determine binding order, the substrate dependence of SdcF transport was measured at two sodium concentrations and sodium dependence was measured at two succinate concentrations. The two sodium and succinate concentrations were chosen based on estimates of $K_{0.5}$ and $V_{max}$. The activation of [$^{14}$C]succinate transport by increasing concentrations of sodium in RSO vesicles containing SdcF is shown in

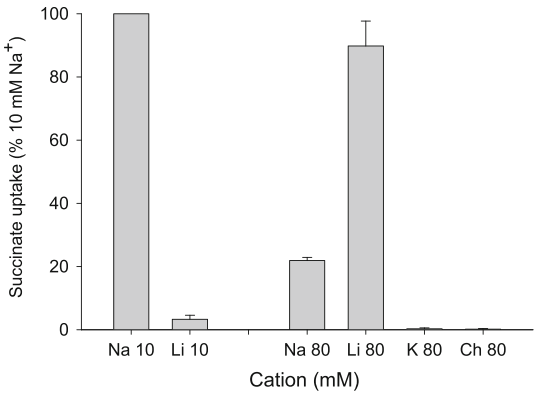


**Fig. 5** Cation specificity of SdcF. Initial rates (30 s) of 20 μM [$^{14}$C]succinate transport in RSO membrane vesicles were measured in buffer containing 80 mM cation (as chloride salts) with 50 mM MOPS, pH 7. The 10 mM $Na^+$ or $Li^+$ treatment groups also contained 70 mM choline Cl. The data have been corrected for background transport in control *E. coli* transformed with pQE-80L vector plasmid. The results shown are data from two independent membrane preparations, normalized to the transport value measured in the presence of 10 mM NaCl + 70 mM choline Cl, and the *error bars* show the range

Fig. 6a. The experiment was done by replacing sodium with choline, up to 10 mM, together with 70 mM choline Cl, for a final cation concentration of 80 mM. The sodium activation was tested in paired experiments at two different succinate concentrations, 10 and 60 μM. As shown in Fig. 6a, the kinetics of sodium activation were sigmoidal, indicating multiple cation binding sites. At 60 μM succinate, the mean Hill coefficient ($n_H$) was 2.44 ± 0.2, the $K_{0.5}$ for $Na^+$ was 0.98 ± 0.1 mM and the $V_{max}$ was 2,305 ± 221 pmol/mg-min (mean ± SEM, $n = 3$). At 10 μM succinate, the mean $n_H$ was 3.23 ± 0.07, the $K_{0.5}$ for $Na^+$ was 1.58 ± 0.1 mM and the $V_{max}$ was 1,212 ± 76 pmol/mg-min (mean ± SEM, $n = 3$). Therefore, the predominant effect of succinate on the sodium activation curves was on $V_{max}$, which is consistent with an ordered binding mechanism in which sodium binds first (Segel 1975; Wright et al. 1983). The sigmoidal sodium activation kinetic curves with Hill coefficients greater than 2 are consistent with at least three sodium ions being involved in transport of succinate. However, the transport appeared electroneutral. There was no difference in transport measured with an outwardly directed gradient of potassium ($[K^+]_{in}$ 100 mM >$[K^+]_{out}$ 20 mM) and equal concentrations of potassium on both sides of the membrane in the presence of 10 μM valinomycin (results not shown), suggesting that SdcF transport is not affected by membrane potential.

The kinetics of succinate transport in RSO vesicles containing SdcF are shown in Fig. 6b, measured at two different sodium concentrations, 1.5 and 10 mM sodium. Similar to our recent findings with SdcS (Pajor and Sun 2013), the succinate transport kinetics appeared to be sigmoidal in SdcF. The kinetic constants under saturating sodium conditions (in 10 mM sodium) were: $K_{0.5}$ for

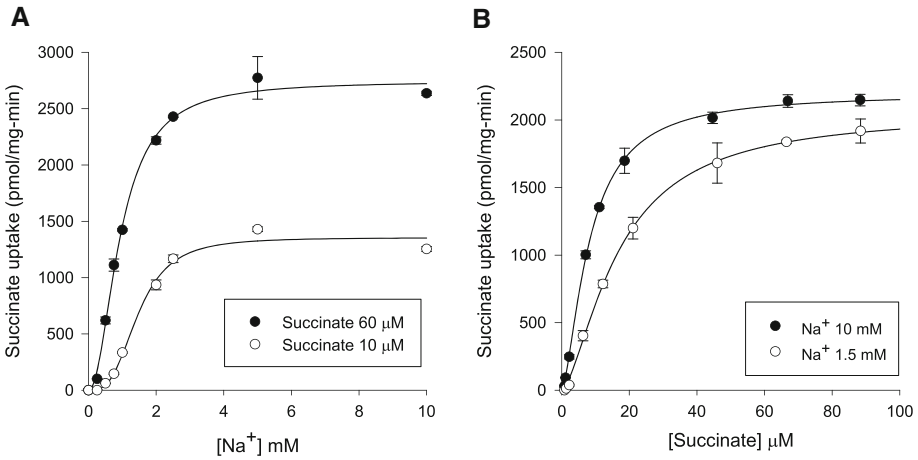


**Fig. 6** Sodium and succinate effects on transport by SdcF. **a** Sodium activation of succinate transport. Initial rates (10 s) of 10 or 60 μM [$^{14}$C]succinate were measured in the same RSO vesicles expressing SdcF in an assay buffer containing 0–10 mM $Na^+$ with up to 80 mM choline Cl, pH 7 ($Na^+$ was replaced by choline). The results shown are from a single preparation, and the *error bars* show the range of duplicate measurements. Kinetic constants in 60 μM succinate: $K_{0.5}$ for sodium 0.9 ± 0.04 mM (mean ± standard error of fit), $V_{max}$ 2,744 ± 62 pmol/mg-min, $n_H$ 2.04 ± 0.16. Kinetic constants in 10 μM succinate: $K_{0.5}$ for $Na^+$ 1.5 ± 0.08 mM, $V_{max}$ 1,355 ± 49 , $n_H$ 3.1 ± 0.38. **b** Succinate kinetics. Initial rates (10 s) of [$^{14}$C]succinate transport were measured in RSO vesicles from *E. coli* expressing SdcF in an assay buffer containing 10 or 1.5 mM $Na^+$ and up to 80 mM choline Cl pH 7 ($Na^+$ was replaced by choline). The *curve* shows a single experiment. Duplicate measurements were done for each data point, and the range is shown by the *error bars*. Kinetic constants in 10 mM $Na^+$: $K_{0.5}$ 8.2 ± 0.2 μM (mean ± standard error of fit), $V_{max}$ 2,196 ± 21 pmol/mg-min, $n_H$ 1.54 ± 0.05. Kinetic constants in 1.5 mM $Na^+$: $K_{0.5}$ 16.8 ± 0.8 μM, $V_{max}$ 2,056 ± 46 pmol/mg-min, $n_H$ 1.53 ± 0.08

succinate 8 ± 1 μM, $V_{max}$ 2,135 ± 161 pmol/mg-min and Hill coefficient 1.58 ± 0.4 (mean ± SEM, $n = 3$). In paired experiments using the same batches of vesicles, the kinetic constants in 1.5 mM sodium were $K_{0.5}$ for succinate 17 ± 1 μM (significantly different $p < 0.05$), $V_{max}$ 2,007 ± 243 pmol/mg-min and Hill coefficient 1.59 ± 0.16 (mean ± SEM, $n = 3$). Therefore, the predominant effect of sodium on succinate kinetics was on $K_{0.5}$ for succinate, also consistent with an ordered binding mechanism in which succinate binds last.

### Lithium-Dependent Succinate Transport

The interaction between SdcF and lithium was also examined. In Fig. 7a, succinate kinetics were measured in 80 mM lithium. The succinate $K_{0.5}$ in lithium was 17 μM, the $V_{max}$ was 2,249 pmol/mg-min and the Hill coefficient was 1.31. In a second experiment with lithium, the $K_{0.5}$ for succinate was 18 μM, the $V_{max}$ was 3,189 pmol/mg-min and the Hill coefficient was 1.14. Lithium also activated [$^{14}$C]succinate transport with sigmoidal kinetics. The concentration range tested was 0–80 mM LiCl, with the lithium replaced by choline. In the experiment shown in Fig. 7b, the Hill coefficient was 1.65 and the $K_{0.5}$ for lithium was 38 mM. In three experiments, the mean Hill coefficient was 2.5 ± 0.6, the $K_{0.5}$ for lithium was 40 ± 9 mM and the $V_{max}$ was 1,680 ± 344 pmol/mg-min. This result shows that lithium can substitute for sodium, but the transporter has a lower affinity for lithium than sodium. The Hill coefficient of 2.5 suggests that three lithium ions may be involved in transport, either as cotransported cations or as allosteric activators. In a separate series of experiments, we tested the activation of succinate transport by higher concentrations of lithium, up to 240 mM, because the experiments up to 80 mM LiCl did not show saturation at the highest concentration. However, the results were inconclusive, possibly because the high-salt experiments had a considerable osmotic gradient (100 mM KPi inside the vesicle and 240 mM LiCl or choline Cl/50 mM MOPS outside). The kinetic curve at 240 mM salt concentration appeared to be shifted to the right compared with the experiments done at 80 mM. In the experiment shown in Fig. 7c, the $K_{0.5}$ for $Li^+$ was 117 mM, $n_H$ was 1.92 and $V_{max}$ was 3,283 pmol/mg-min. In three experiments, the mean kinetic values were $K_{0.5}$ for $Li^+$ 97 ± 18 mM, $n_H$ 1.7 ± 0.3 and $V_{max}$ 3,270 ± 467 pmol/mg-min.

## Discussion

The present study reports the functional characterization of SdcF from *B. licheniformis*, a new member of the DASS/SLC13 family. To date, three additional bacterial DASS family members have been functionally characterized: SdcL from *B. licheniformis* (Strickler et al. 2009), SdcS from *S. aureus* (Hall and Pajor 2005, 2007; Joshi and Pajor 2009) and DccT from *C. glutamicum* (Youn et al. 2008). The amino acid sequences of the four transporters are approximately 40–50 % identical to one another, and they are ~30 % identical to the mammalian SLC13/DASS transporters, such as the human NaDC1 (Pajor 1996). The prokaryotic DASS transporters are all sodium-coupled and carry four-carbon dicarboxylate substrates. However, lithium can substitute equally well for sodium in transporting succinate in SdcF.

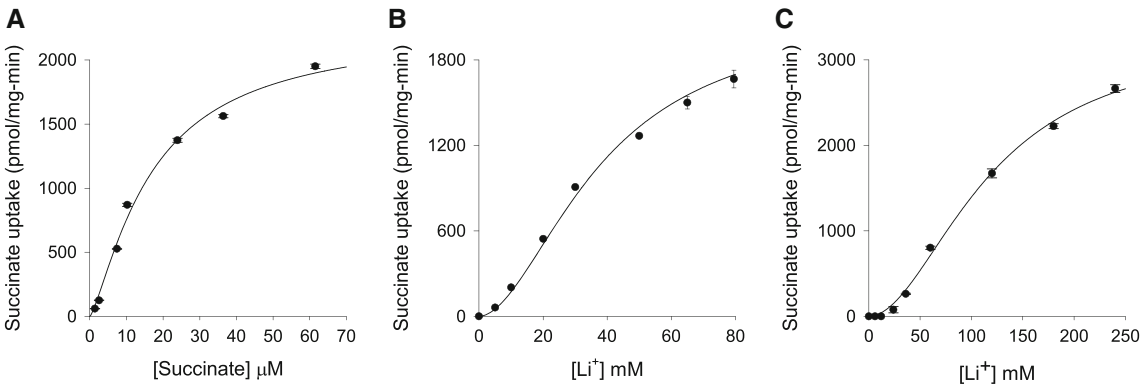


**Fig. 7** Effects of lithium on succinate transport by SdcF. **a** Succinate kinetics. Initial rates (10 s) of [$^{14}$C]succinate transport were measured in RSO membrane vesicles expressing SdcF in buffers containing 80 mM LiCl. Duplicate measurements were done for each data point, and the range is shown by the *error bars*. Kinetic constants were $K_{0.5}$ 17 ± 4 μM, $V_{max}$ 2,249 ± 258 pmol/mg-min, $n_H$ 1.31 ± 0.21 (mean ± standard error of fit). **b** Lithium activation of succinate transport up to 80 mM LiCl. Initial rates of 20 μM [$^{14}$C]succinate transport were measured in RSO membrane vesicles expressing SdcF in buffers containing up 80 mM LiCl ($Li^+$ was replaced by choline). Kinetic constants were $K_{0.5}$ 38 ± 4 mM, $V_{max}$ 2,131 ± 149 pmol/mg-min, $n_H$ 1.64 ± 0.13 (mean ± standard error of fit). **c** Lithium activation of succinate transport up to 240 mM LiCl. Initial rates of 20 μM [$^{14}$C]succinate transport were measured in RSO membrane vesicles expressing SdcF in buffers containing up 240 mM LiCl ($Li^+$ was replaced by choline). Kinetic constants were $K_{0.5}$ 117 ± 12 mM, $V_{max}$ 3,282 ± 255 pmol/mg-min, $n_H$ 1.92 ± 0.17 (mean ± standard error of fit)

SdcF transports the four-carbon dicarboxylate succinate as well as the five-carbon AKG. Succinate transport by SdcF was inhibited by four-carbon dicarboxylates including succinate (butanedioic acid), malate (2-hydroxy butanedioic acid), fumarate, tartrate (2,3-OH butanedioic acid) and OAA (2-oxo butanedioic acid). In addition, the four-carbon amino acid L-aspartate inhibited transport, whereas the addition of an acetyl group (*N*-acetyl aspartate) resulted in a less effective inhibitor of succinate transport by SdcF in RSO membrane vesicles. Taken together, the results of the present study suggest that SdcF can tolerate substitutions at positions C2 and C3 of succinate. SdcF appeared to have a low affinity for α-ketoglutarate and did not transport larger substrates, such as citrate. The substrate specificity profile of SdcL, also from *B. licheniformis*, was very similar to that of SdcF (Strickler et al. 2009); and the present study showed that both transporters were inhibited by tartrate. DccT and SdcS have substrate profiles that are similar to those of SdcF and SdcL (Hall and Pajor 2005; Youn et al. 2008), with the exception of tartrate, which was not an effective inhibitor of succinate transport in DccT or SdcS. A previous study on the *C. glutamicum* DccT observed strong inhibition of succinate transport by oxaloacetate, the first report of a noneukaryotic transporter for OAA (Youn et al. 2008). In the present study, we found that OAA inhibited SdcF, as well as SdcS and SdcL (unpublished observations, results not shown), suggesting that transport of OAA may be a feature of the DASS transporters.

The high-resolution crystal structure of the *V. cholerae* $Na^+$/dicarboxylate transporter VcINDY was recently solved in an inward-facing conformation (Mancusso et al. 2012). The structure of the protein consists of a new protein fold with an inverted twofold symmetry of transmembrane helices TM2-6 and TM7-11. The key domains for binding substrate and cations are located in the two opposing helical hairpin structures, $HP_{in}$ and $HP_{out}$, and in the unwound portions of helices TM5 and TM10. These regions are highly conserved among the bacterial DASS transporters (see sequence alignment, Fig. 1). For example, 17–19 amino acid stretches of $HP_{in}$ or $HP_{out}$ are ~50 % identical among the bacterial DASS transporters, and an 18 amino acid segment of TM10 is 67 % identical. Interestingly, the VcINDY transporter appears to interact with citrate: the crystal structure contained citrate in the substrate binding site, and citrate inhibited succinate transport by ~20 % (Mancusso et al. 2012). In contrast, the other bacterial DASS transporters do not interact with citrate and the preferred substrates are four-carbon dicarboxylates (Hall and Pajor 2005; Strickler et al. 2009; Youn et al. 2008). However, the key substrate binding residues in $HP_{in}$ and $HP_{out}$ make contacts with only two out of the three carboxyl groups of citrate (Mancusso et al. 2012), and these residues are conserved among the bacterial DASS transporters (Fig. 1). For example, Ser-150 and Asn-151 in $HP_{in}$ of VcINDY (Ser-140 and Asn-141 of SdcF) are predicted to interact with both carboxyl-5 of citrate and one sodium ion (Mancusso et al. 2012). Similarly, in $HP_{out}$, Ser-385 and Asn-386 of SdcF correspond with Ser-377 and Asn-378 of VcINDY, also predicted to interact with substrate. The conserved threonine at position 379 in VcINDY (Thr-387 in SdcF) was shown to determine substrate selectivity between succinate and sulfate (Mancusso et al. 2012). Although the bacterial DASS transporters prefer four-carbon dicarboxylate substrates, the eukaryotic $Na^+$/dicarboxylate transporters NaDC1, NaDC3 and NaCT all transport citrate in addition to four-carbon dicarboxylates (Inoue et al. 2002; Kekuda et al. 1999; Pajor et al. 2001; Yao and Pajor 2000).

The SdcF transporter characterized in the present study had a relatively high substrate affinity, with a $K_{0.5}$ for succinate of around 8–17 μM, similar to the 6 μM $K_m$ for succinate in SdcL (Strickler et al. 2009). DccT in intact *C. glutamicum* has a succinate $K_m$ of 30 μM (Youn et al. 2008). The succinate $K_m/K_{0.5}$ in SdcS is 6–26 μM, depending on the preparation (Hall and Pajor 2005, 2007; Joshi and Pajor 2009). Interestingly, succinate kinetics in SdcF appeared sigmoidal rather than hyperbolic. The Hill coefficient was around 1.6, suggesting that there are at least two interacting substrate binding sites. Similarly, the Hill coefficients reported in DccT for succinate and fumarate are greater than 2 and 1.3 with malate (Youn et al. 2008). Furthermore, our recent study of SdcS showed that succinate kinetics are also sigmoidal in that transporter, with a Hill coefficient for succinate of around 1.3 (Pajor and Sun 2013). Therefore, the results raise the possibility that some or all of the bacterial members of the DASS family contain multiple cooperative substrate binding sites, either on the same subunit or as a result of interaction of multiple subunits. The recent crystal structure of VcINDY shows a dimeric protein (Mancusso et al. 2012), although experiments are needed to determine whether the dimer is the functional unit. The GLUT1 glucose transporter is an example of a transporter with multiple interacting substrate binding sites on different subunits (Robichaud et al. 2011). There is also precedence for allosteric substrate binding sites in other transporters. For example, CaiT, the carnitine/butyrobetaine antiporter from *Proteus mirabilis*, has an allosteric substrate binding site that regulates the transport rate (Schulze et al. 2010). The neurotransmitter transporter homolog LeuT has a second high-affinity substrate binding site which is involved in the transport cycle. Release of the transported substrate and sodium ion is thought to be triggered by substrate binding to the second substrate binding site (Quick et al. 2012).

Most of the dicarboxylate transporters of the DASS/SLC13 family are sodium-coupled transporters that use the

energy from the inwardly directed sodium gradient across the cell membrane to drive concentrative transport of dicarboxylate substrates. The mammalian members of the family couple three or four sodium ions to the transport of substrate and have $K_{0.5}$ values for sodium of approximately 20–40 mM (Inoue et al. 2004; Pajor et al. 1998). By comparison, the bacterial SdcS and SdcL transporters appear to couple two sodium ions to the transport of each succinate and have high affinities for sodium with $K_{0.5}$ values of 2.7 mM (SdcS) and 0.8 mM (SdcL) (Hall and Pajor 2005; Strickler et al. 2009). DccT also had a high sodium affinity, with a $K_{0.5} \sim 1$ mM (Youn et al. 2008). Similarly, succinate transport by SdcF in the present study was stimulated by sodium with sigmoidal kinetics. The $K_{0.5}$ for sodium was around 1–1.6 mM, and the mean Hill coefficient for sodium activation was greater than 2, which is consistent with at least three sodium ions involved in transport.

The coupled transport of sodium and succinate by SdcF appears to follow an ordered binding mechanism in which sodium binds first and succinate binds last (Segel 1975). Sodium is an essential activator of succinate transport, and there was no transport activity in the absence of sodium. The sodium activation kinetic curves were affected by succinate concentration, with a lower $V_{max}$ at the lower succinate concentration. In succinate kinetic experiments, the $K_{0.5}$ for succinate was affected by sodium but there was no significant change in $V_{max}$ at different sodium concentrations. This result supports the model that succinate binds last to SdcF. The mammalian SLC13 transporters also appear to follow an ordered binding mechanism in which three $Na^+$ are bound first, followed by one divalent anion substrate and the net transfer of one positive charge across the membrane (Wright et al. 1983; Yao and Pajor 2000). The mechanism of SdcF transport may be somewhat different from that of the mammalian transporters. SdcF transport appears to be electroneutral, and the sigmoid substrate kinetic curve suggests multiple interacting substrate binding sites. If the transporting unit of SdcF is a dimer, as suggested by the VcINDY crystal structure (Mancusso et al. 2012), then the results are consistent with cooperativity between protomers that each bind two $Na^+$ and one $succinate^{2-}$, for a net stoichiometry of 4 $Na^+$:2 $succinate^{2-}$. However, if a single subunit is the transporting unit, the results could be explained by the electroneutral transport of 2 $Na^+$:1 $succinate^{2-}$ with additional allosteric binding sites for nontransported $Na^+$ and $succinate^{2-}$. Clearly, it will be important to determine the number of subunits involved in transport by SdcF.

Although many of the sodium-dependent DASS/SLC13 family members also bind lithium, typically lithium does not produce the optimal conformational change to allow high-affinity substrate binding. In the rabbit NaDC1, for example, the $K_m$ for succinate is tenfold higher in lithium than in sodium (Pajor et al. 1998). Some members of the family exhibit transport inhibition in the presence of both sodium and lithium, due to binding of lithium to one high-affinity cation binding site (Pajor et al. 1998). In the present study, SdcF was stimulated by lithium with sigmoid kinetics and a Hill coefficient of 2.5, indicating that at least three cation binding sites bind lithium. The relative affinity for lithium was lower than that for sodium, however, with a $K_{0.5}$ for $Li^+$ of 38 mM compared with a $K_{0.5}$ of 1.5 mM for $Na^+$. Under high cation concentrations (10 mM $Na^+$ or 80 mM $Li^+$), the succinate kinetics were virtually identical in both sodium and lithium with similar $K_{0.5}$ and $V_{max}$ values. The other *B. licheniformis* DASS member, SdcL, may also transport succinate coupled with lithium because the rate of succinate transport in 80 mM $Li^+$ was approximately the same as in 10 mM $Na^+$ (unpublished observations, not shown). In contrast, although SdcS can also use lithium to drive succinate transport, the maximum transport rate is about 40 % of that in sodium (Hall and Pajor 2005). The results suggest that the cation binding sites in SdcF may be slightly different from those in the other members of the family to allow the smaller lithium cation to drive transport (Gouaux and Mackinnon 2005). Lithium-coupled transport has also been reported for prokaryotic transporters for proline and melibiose, but these transporters are not related to the DASS family (Chen et al. 1985; Tsuchiya et al. 1983). VcINDY has high succinate transport activity in 5 mM $Li^+$, suggesting a similar high affinity for both sodium and lithium, although this has not yet been characterized in detail (Mancusso et al. 2012).

In conclusion, this study describes the functional properties of the SdcF transporter from *B. licheniformis*. SdcF is a DASS family member, approximately 40–50 % identical to the other bacterial DASS transporters. The functional properties of SdcF were very similar to those of the second DASS family member in *B. licheniformis*, SdcL. The physiological roles of the two dicarboxylate transporters in *B. licheniformis* are not known at present. SdcF transports four- and five-carbon dicarboxylates together with sodium or lithium ions. In addition, there appear to be two interacting substrate binding sites, indicating either an allosteric regulatory site or interaction between substrate binding sites on multiple subunits of the transporter. Finally, the kinetic experiments are consistent with an ordered binding model in which the sodium ions bind first and the succinate binds last.

**Acknowledgments** Most of this work was supported by grant DK46269 from the National Institutes of Health (to A. M. P.). Jason Hall originally identified the SdcF sequence as a closely related DASS family member. Thanks to Shelly Peng and Ereca Nguyen for preparing media and solutions.

## References


Chen CC, Tsuchiya T, Yamane Y, Wood JM, Wilson TH (1985) $Na^+$ ($Li^+$)-proline cotransport in *Escherichia coli*. J Membr Biol 84:157–164

Ebbighausen H, Weil B, Kramer R (1991) $Na^+$-dependent succinate uptake in *Corynebacterium glutamicum*. FEMS Microbiol Lett 61:61–65

Gouaux E, Mackinnon R (2005) Principles of selective ion transport in channels and pumps. Science 310:1461–1465

Hall JA, Pajor AM (2005) Functional characterization of a $Na^+$-coupled dicarboxylate carrier protein from *Staphylococcus aureus*. J Bacteriol 187:5189–5194

Hall JA, Pajor AM (2007) Functional reconstitution of SdcS, a $Na^+$-coupled dicarboxylate carrier protein from *Staphylococcus aureus*. J Bacteriol 189:880–885

Huang W, Wang H, Kekuda R, Fei YJ, Friedrich A, Wang J, Conway SJ, Cameron RS, Leibach FH, Ganapathy V (2000) Transport of *N*-acetylaspartate by the $Na^+$-dependent high-affinity dicarboxylate transporter NaDC3 and its relevance to the expression of the transporter in the brain. J Pharmacol Exp Ther 295:392–403

Inoue K, Zhuang L, Maddox DM, Smith SB, Ganapathy V (2002) Structure, function and expression pattern of a novel sodium-coupled citrate transporter (NaCT) cloned from mammalian brain. J Biol Chem 277:39469–39476

Inoue K, Fei YJ, Zhuang L, Gopal E, Miyauchi S, Ganapathy V (2004) Functional features and genomic organization of mouse NaCT, a sodium-coupled transporter for tricarboxylic acid cycle intermediates. Biochem J 378:949–957

Joshi AD, Pajor AM (2009) Identification of conformationally sensitive amino acids in the $Na^+$/dicarboxylate symporter (SdcS). Biochemistry 48:3017–3024

Kekuda R, Wang H, Huang W, Pajor AM, Leibach FH, Devoe LD, Prasad PD, Ganapathy V (1999) Primary structure and functional characteristics of a mammalian sodium-coupled high affinity dicarboxylate transporter. J Biol Chem 274:3422–3429

Mancusso R, Gregorio GG, Liu Q, Wang DN (2012) Structure and mechanism of a bacterial sodium-dependent dicarboxylate transporter. Nature 491:622–627

Pajor AM (1995) Sequence and functional characterization of a renal sodium/dicarboxylate cotransporter. J Biol Chem 270:5779–5785

Pajor AM (1996) Molecular cloning and functional expression of a sodium-dicarboxylate cotransporter from human kidney. Am J Physiol Renal Physiol 270:F642–F648

Pajor AM (2006) Molecular properties of the SLC13 family of dicarboxylate and sulfate transporters. Pflugers Arch 451:597–605

Pajor AM, Randolph KM (2005) Conformationally sensitive residues in extracellular loop 5 of the $Na^+$/dicarboxylate co-transporter. J Biol Chem 280:18728–18735

Pajor AM, Sun NN (2013) NSAIDS and other anthranilic acids inhibit the $Na^+$/dicarboxylate symporter from *S. aureus* (SdcS). Biochemistry 52(17):2924–2932

Pajor AM, Hirayama BA, Loo DDF (1998) Sodium and lithium interactions with the $Na^+$/dicarboxylate cotransporter. J Biol Chem 273:18923–18929

Pajor AM, Gangula R, Yao N (2001) Cloning and functional characterization of a high-affinity $Na^+$/dicarboxylate cotransporter from mouse brain. Am J Physiol Cell Physiol 280:C1215–C1223

Prakash S, Cooper G, Singhi S, Saier MH Jr (2003) The ion transporter superfamily. Biochim Biophys Acta 1618:79–92

Quick M, Yano H, Goldberg NR, Duan L, Beuming T, Shi L, Weinstein H, Javitch JA (2006) State-dependent conformations of the translocation pathway in the tyrosine transporter Tyt1, a novel neurotransmitter:sodium symporter from *Fusobacterium nucleatum*. J Biol Chem 281:26444–26454

Quick M, Shi L, Zehnpfennig B, Weinstein H, Javitch JA (2012) Experimental conditions can obscure the second high-affinity site in LeuT. Nat Struct Mol Biol 19:207–211

Rey MW, Ramaiya P, Nelson BA, Brody-Karpin SD, Zaretsky EJ, Tang M, de Lopez LA, Xiang H, Gusti V, Clausen IG, Olsen PB, Rasmussen MD, Andersen JT, Jorgensen PL, Larsen TS, Sorokin A, Bolotin A, Lapidus A, Galleron N, Ehrlich SD, Berka RM (2004) Complete genome sequence of the industrial bacterium *Bacillus licheniformis* and comparisons with closely related *Bacillus* species. Genome Biol 5:R77

Robichaud T, Appleyard AN, Herbert RB, Henderson PJ, Carruthers A (2011) Determinants of ligand binding affinity and cooperativity at the GLUT1 endofacial site. Biochemistry 50:3137–3148

Schulze S, Koster S, Geldmacher U, Terwisscha van Scheltinga AC, Kuhlbrandt W (2010) Structural basis of $Na^+$-independent and cooperative substrate/product antiport in CaiT. Nature 467:233–236

Segel IH (1975) Enzyme kinetics. John Wiley and Sons, New York

Strickler MA, Hall JA, Gaiko O, Pajor AM (2009) Functional characterization of a $Na^+$-coupled dicarboxylate transporter from *Bacillus licheniformis*. Biochim Biophys Acta 1788:2489–2496

Teramoto H, Shirai T, Inui M, Yukawa H (2008) Identification of a gene encoding a transporter essential for utilization of C4 dicarboxylates in *Corynebacterium glutamicum*. Appl Environ Microbiol 74:5290–5296

Tsuchiya T, Oho M, Shiota-Niiya S (1983) Lithium ion–sugar cotransport via the melibiose transport system in *Escherichia coli*: measurement of $Li^+$ transport and specificity. J Biol Chem 258:12765–12767

Williams CM, Richter CS, Mackenzie JM, Shih JC (1990) Isolation, identification, and characterization of a feather-degrading bacterium. Appl Environ Microbiol 56:1509–1515

Wright SH, Hirayama B, Kaunitz JD, Kippen I, Wright EM (1983) Kinetics of sodium succinate cotransport across renal brush-border membranes. J Biol Chem 258:5456–5462

Yao X, Pajor AM (2000) The transport properties of the human renal $Na^+$/dicarboxylate cotransporter under voltage clamp conditions. Am J Physiol Renal Fluid Electrolyte Physiol 279:F54–F64

Youn JW, Jolkver E, Kramer R, Marin K, Wendisch VF (2008) Identification and characterization of the dicarboxylate uptake system DccT in *Corynebacterium glutamicum*. J Bacteriol 190:6458–6466